

Real-space Observation of Incommensurate Spin Density Wave and Coexisting Charge Density Wave on Cr(001) surface

Yining Hu^{1†}, Tianzhen Zhang^{1†}, Dongming Zhao¹, Chen Chen¹, Shuyue Ding¹, Wentao Yang¹, Xu Wang¹, Chihao Li¹, Haitao Wang¹, Tong Zhang^{1,3,4*}, Donglai Feng^{2,3,4}

¹ State Key Laboratory of Surface Physics, Department of Physics, and Advanced Materials Laboratory, Fudan University, Shanghai 200438, China

² Hefei National Laboratory for Physical Science at Microscale and Department of Physics, University of Science and Technology of China, Hefei, Anhui 230026, China

³ Collaborative Innovation Center of Advanced Microstructures, Nanjing 210093, China

⁴ Shanghai Research Center for Quantum Sciences, Shanghai 201315, China

† These authors contributed equally.

Via spin-polarized scanning tunneling microscopy, we revealed a long-range ordered spin density wave (SDW) for the first time on a Cr (001) surface, corresponding to the well-known incommensurate SDW of bulk Cr. It displays a (~ 6.0 nm) long-period spin modulation in each (001) plane and an anti-phase behavior between adjacent planes, which are confirmed by changing the magnetization of the tip. Meanwhile, we simultaneously observed the coexisting charge density wave (CDW) with half the period of the SDW. Taking advantage of real-space measurement, we found the charge and spin modulations are in-phase, and their domain structures are highly correlated. Surprisingly, the phase of CDW in dI/dV map displays a π shift around a density-of-states dip at about -22 meV, indicating an anomalous CDW gap opened *below* E_F . These observations support that the CDW is a secondary order driven by SDW. Therefore, our work is not only the first real space characterization of incommensurate SDW, but also provide new insights on how SDW and CDW coexist.

A spin density wave (SDW) state manifests itself as real-space spin modulations. It is usually formed in itinerant magnetic systems with Fermi surface nesting and electron-electron interactions [1]. The spatial period of SDW could be commensurate (C-SDW) or incommensurate (IC-SDW) to lattice constant. In the latter case, the spin modulation decouples from lattice, which is distinguished from local moment induced anti-ferromagnetic (AFM) order. Interestingly, SDW often coexists and sometimes intertwines with other orders in correlated systems, such as charge density wave (CDW) and superconductivity [1-4]. The interplay of these coexisting/intertwining orders has now become an important theme in condensed matter physics. To date, the commonly observed SDW states are commensurate SDW, such as the collinear/bicollinear SDW (AFM) state in iron-based superconductors [4,5]; while incommensurate SDW is rarely seen, and particularly, its real space imaging is quite

lacking.

Chromium (Cr) is one of the classic examples which shows itinerant magnetism with an IC-SDW ground state [6-8]. Such IC-SDW is stabilized by “imperfect” Fermi surface nesting condition [8], as illustrated in Fig. 1(a). Specifically, the Fermi surfaces of Cr (b.c.c. lattice) are composed of hole pockets at the corner and electron pocket at the center of the Brillouin zone [6]. The hole pocket is slightly larger than the electron pocket which yields two nesting vectors: $Q_{\pm} = 2\pi/a (1\pm\delta)$ ($a = 2.9$ Å being the lattice constant). Therefore, a long period IC-SDW with a wave vector $Q_{SDW} = 2\pi\delta/a$ is generated which overlaps with the AFM coupling between Cr atoms (Fig. 1(b)). The wavelength of IC-SDW is reported to be ~ 6.0 nm at $T < 10$ K ($\delta \sim 0.05$) [10], and Q_{SDW} is along equivalent $\langle 001 \rangle$ directions. The spin orientation of Cr atom is found to be perpendicular to Q_{SDW} at $T > T_{SF}$ (123 K) but switched to be parallel at $T < T_{SF}$ (spin-flip transition [6]).

In addition to IC-SDW, a charge density wave (CDW) with half period of the IC-SDW was also found in Cr [10~13]. Unlike the IC-SDW, the exact origin of such CDW is yet to be understood. It was often considered as the second-order harmonics of IC-SDW [12], corresponding to a nesting vector $Q_{CDW} = 2Q_{SDW}$ that connects the two folded bands at Γ (Fig. 1(a)); alternatively, it was suggested as a lattice strain wave induced by magneto-elastic coupling to the IC-SDW [6]. Therefore, being a pure element arranged in a simple structure, Cr is also a classical system to study the interplay of SDW/CDW orders.

However, after decades of research, the characterization of IC-SDW (and CDW) in Cr is still rather limited to spatially averaged method, such as neutron scattering [6,7], x-ray diffraction [10,13] and photoemission spectroscopy [14,15]. In principle, SDW could also be detected by local probes at atomic scale, such as spin-polarized scanning tunneling microscopy (SP-STM) [16]. Although a few SP-STM studies have been performed on various Cr surfaces [17-26], the real-space evidence of IC-SDW was rarely reported (some studies found CDW modulation in Cr (110) [23, 27], and argued the satellite FFT spots as an indication of IC-SDW [23]). Most SP-STM studies on Cr (001) surface only observed in-plane ferromagnetism with AFM coupling between adjacent (001) planes [17-22]. To understand such a ferromagnetic spin arrangement on surface, it was suggested the magnetic moment is enhanced at the surface [28] and the IC-SDW antinodes are always pinned on the surface [8,19], making it invisible to STM. However, we notice that most previous STM studies on Cr (001) did not resolve clear atomic lattices, although mono-atomic terrace can be identified. This is likely due to local disorders induced by segregated impurities on the surface, which is a common problem in cleaning Cr single crystal sample. As the surface conditions could alter the surface magnetism [8], it would be intriguing to search the IC-SDW in real space again on a well-ordered Cr surface.

In this work, by using low-temperature spin-polarized STM with vector magnetic field, we studied a thoroughly cleaned Cr (001) surface with a well-ordered $c(2\times 2)$ reconstruction. For the first time, we observed clear spin modulation with a period of 6.0 nm, propagating along in-plane [100] or [010] directions, which well matches the projected bulk IC-SDW on (001)

surface. Its SDW nature is confirmed by the contrast inversion upon switching tip's magnetization, and the anti-phase relation between adjacent terraces. Meanwhile, we also observed the coexisting CDW with a period 3.0 nm, and surprisingly found that it displays a π phase shift around gap structure about 22 meV *below* E_F , which suggests its formation is beyond the intuitive Fermi surface nesting picture. Furthermore, as a local probe measurement, we directly observed the domain structure of SDW/CDW and revealed their in-phase relation. Our work not only gives the first real space investigation of IC-SDW, but also provide new insights on the general mechanism of coexisting SDW/CDW orders.

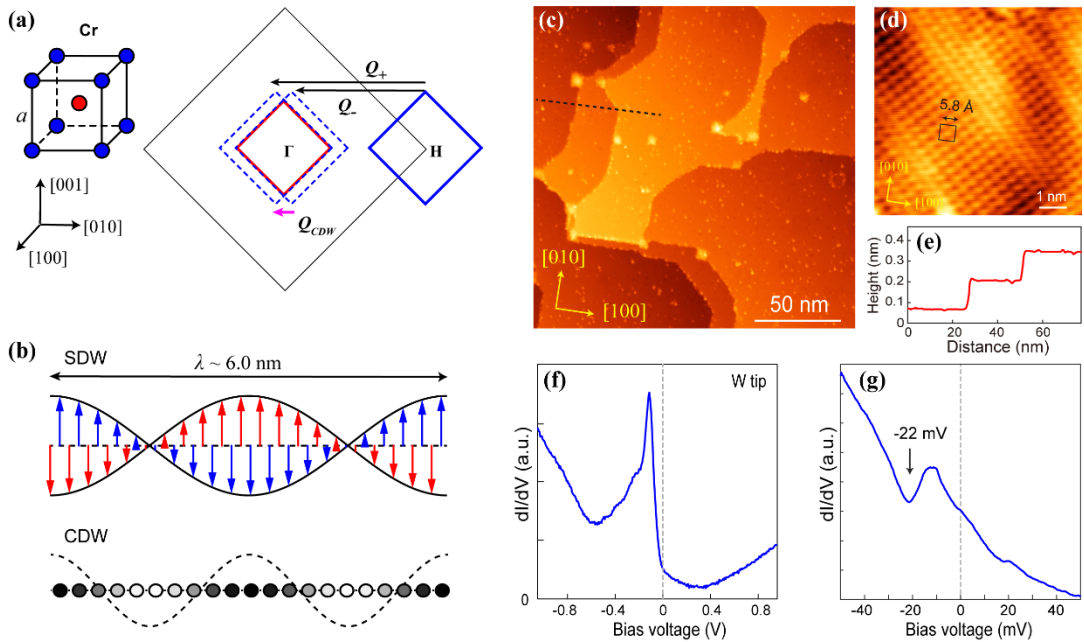


Figure 1 (a): Left: the body-centered cubic (b.c.c.) structure, and right: the (001) plane Brillouin zone of Cr. Electron and hole Fermi surfaces (cross sections) are represented by red and blue squares, respectively. The nesting vectors $Q_{\pm} = 2\pi/a (1 \pm \delta)$ are indicated by black arrows, and $Q_{CDW} = Q_+ - Q_-$ is the CDW wave vector. (b) Schematic of incommensurate SDW and CDW of bulk Cr in real space. Blue and red arrows represent the spin of corner and body-center Cr atoms in the b.c.c. lattice (at $T > T_{SF}$), respectively. Solid (hollow) circles represent the locations with the highest (lowest) charge density. (c) Large scale STM image (190×190 nm²) of the cleaned Cr (001) surface. (d) Atomically resolved STM image, which shows the centered (2×2) structure. (e) Line profile taken along the dashed line in panel (c). (f) Typical dI/dV spectrum taken on defect-free region with a normal W tip (setpoint: $V_b = 1$ V, $I = 60$ pA). (g) dI/dV spectrum near E_F (setpoint: $V_b = 100$ mV, $I = 100$ pA), a DOS dip around $V_b = -22$ mV is observed.

The experiment was conducted in a cryogenic STM from UNISOKU at $T = 5.0$ K. Cr (001) single crystal (Mateck, purity: 99.999%) was intensively cleaned by repeated cycles of Ar sputtering at 750°C (for 15 min) and annealing at ~800°C (for 20 min), until a well-ordered surface is obtained. Spin-resolved tunneling spectroscopy and conductance mapping were performed by Cr and Fe coated STM tips, which are prepared by depositing 40 nm Cr or 16 nm Fe layers on W tip. The W tip was electrochemically etched and flashed up to ~2000K for

cleaning before coating. The tunneling conductance (dI/dV) was collected by standard lock-in method and the bias voltage (V_b) is applied to the sample.

Fig. 1(c) shows a large scale STM image of the obtained Cr(001) surface. It displays atomically flat terraces with mono-atomic height (~ 0.14 nm), as indicated by the line profile in Fig. 1(e). It is notable that the terrace edges prefer running along high symmetric directions such as [100], [010] and [110]. This is an indication of free surface atom diffusion during annealing [29]. Despite some randomly distributed defects, atomic lattice can be easily resolved in defect free area, as shown in Fig. 1(d). It displays a centered 2×2 (or $\sqrt{2}\times\sqrt{2}$ R45°) lattice with respect to the pristine Cr 1×1 lattice. We noticed some STM works on Cr (001) also observed $c(2\times 2)$ structures [22,26,30], but the electronic states of the present surface (shown below) is quite different from these studies. Although the origin of this reconstruction is unclear at this stage, it is the first time to observe regular oriented terrace edges with well-ordered lattice on a sputtered/annealed Cr (001) surface.

The typical large energy scale dI/dV spectrum of the surface, taken by a normal W tip above defect-free area, is shown in Fig. 1(f). There is a pronounced DOS peak located at -75 (± 5) meV. We note although a DOS peak was widely observed on Cr surfaces [18-26, 31-32], the peak position varies significantly for different studies. The origin of such a peak was usually attributed to spin-polarized surface state [31,33-35] or the orbital Kondo effect [32]. Our measurements shown below tend to support the former scenario. By zooming into a narrower energy range near E_F (Fig. 1(g)), we found there is an additional DOS dip at $E = -22(\pm 1)$ meV, which has never been reported before. We will show later that this is an energy gap associated with the CDW order, but it opens *below* the Fermi level.

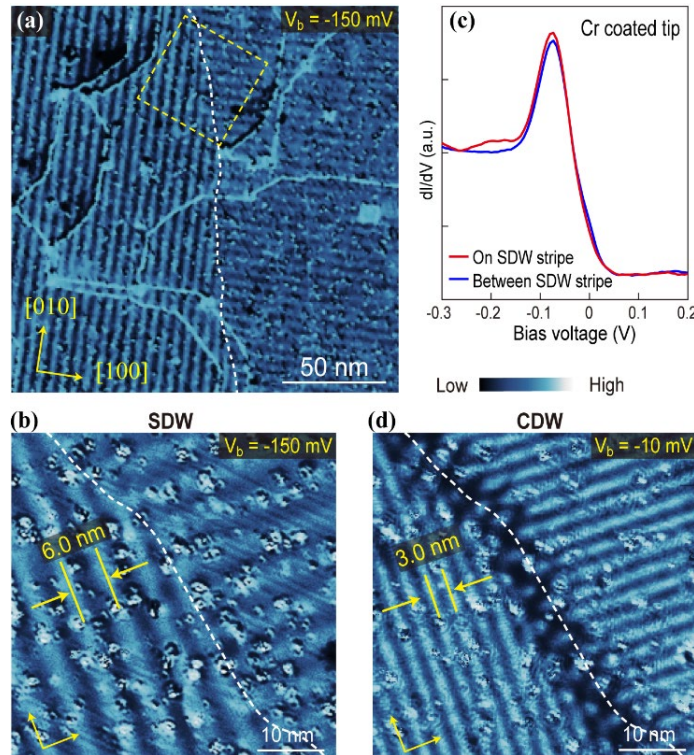


Figure 2. Spin and charge modulations observed on Cr (001) surface (a) dI/dV mapping of the same area that shown in Fig. 1(c), taken by a Cr coated spin-polarized tip at $V_b = -150$ mV ($I = 80$ pA, $\Delta V = 20$ mV). (b) A zoom-in dI/dV map of the marked square in panel (a), which shows spin modulation with a period of 6.0 nm. White dashed line tracks the domain wall ($I = 150$ pA, $\Delta V = 15$ mV). (c) Typical dI/dV spectra taken above and in between the spin modulation stripes. (d) dI/dV map of the same area as (b), but taken at $V_b = -10$ mV. The charge modulation with a period of 3.0 nm is shown ($I = 150$ pA, $\Delta V = 5$ mV).

We then studied the surface with spin-polarized tips. Fig. 2(a) is a dI/dV map taken at $V_b = -150$ meV with a tip coated with 40 nm thick Cr, which favors an in-plane spin polarization [16]. The mapping area is the same as that shown Fig. 1(c). It is remarkable that stripe-like modulations can be observed, and there are two domains of such modulation which are perpendicular to each other. A zoomed-in dI/dV map around a domain wall is shown in Fig. 2(b). The period of the stripe is 6.0 nm and the wave vector is either along [010] or [100] direction. Such a period and propagating direction exactly match the projected bulk IC-SDW of Cr on a (001) surface. It is also seen that the domain walls in Fig. 2(a) (dashed curve) has no correlation with surface morphology (Fig. 1(c)), which indicates the stripes are not merely surface effects but of bulk origin. Fig. 2(c) shows the typical dI/dV spectra taken on the stripe and between the stripes with the Cr coated tip. There is observable difference on the intensity around the DOS peak, which is attributed to spin contrast as discussed below. A series of dI/dV maps taken at different energies can be found in Fig. S1 of the supplementary materials (SM).

To confirm these stripes are spin modulations, we performed measurement with a 16 nm-Fe-coated tip whose magnetization can be controlled by an external magnetic field [16]. Fig. 3(a) and 3(b) are two dI/dV maps taken in the same region, but under opposite in-plane field of $B_x = \pm 1$ T (X direction is perpendicular to stripes, as marked in figure). The 6.0 nm period stripes can be seen in both Fig. 3(a) and 3(b), while they display a clear phase inversion, as further illustrated in their line profiles in Fig. 3(c). Since the tip magnetization will follow such in-plane field, this gives a direct evidence that the stripes are SDW modulations, with opposite spin orientations on their peaks and troughs. We can also tune the tip magnetization along Y and Z directions (by applying $B_y = 1$ T and $B_z = 1.5$ T, respectively), the resulting dI/dV maps are shown in Figs. 3(c) and 3(d), respectively. In these two cases, the contrast of the stripes was significantly reduced and almost invisible. Therefore, the local spins are along X direction, same as the direction of Q_{SDW} . This also agrees with bulk measurements that the IC-SDW is longitudinal wave at $T < T_{\text{SF}}$ [6]. We can extract the spin-polarization ratio (spin-contrast) of Figs. 3(a,b) by calculating their relative intensity difference, which is about 4% at the SDW peaks (Fig. 3(f)). We note here that for Cr coated tip used in Fig. 2, its (in-plane) polarization direction is arbitrary [16], that is why the two SDW domains in Fig. 2(a, b) can be simultaneously imaged but their contrasts are different.

Another signature of IC-SDW can be obtained near the atomic step edges. Fig. 3(g) shows a topographic image of three adjacent mono-atomic height terraces, and Fig. 3(h) is the

corresponding dI/dV map measured by a Cr tip. As shown by dashed lines, there is a phase inversion of the modulations between adjacent terraces. This indicates the local spin of two adjacent (001) plane are still AFM coupled. Based on above observations, we now achieve a complete spin configuration of the present Cr (001) surface. As illustrated in Fig. 3(i), the Cr have an out-of-plane AFM configuration with the spins lie in-plane, while a long wavelength, longitudinal IC-SDW ($\lambda = 6.0$ nm) is present in each (001) planes. Such a magnetic structure is fully consistent with the neutron-scattering measurement for bulk Cr and thick Cr films [6], but only visualized by a local probe for the first time here. Comparing with the commensurate SDW or AFM state [4,16], the IC-SDW observed here are pure spin modulations that decoupled from the lattice.

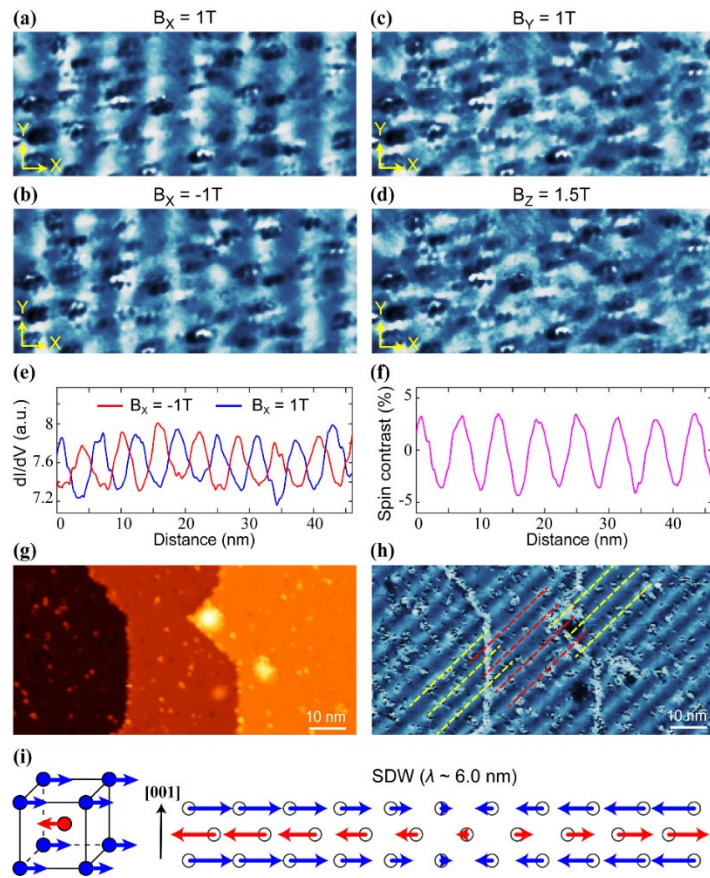


Figure 3. Verifying the nature of spin density wave. (a~d) dI/dV maps taken with a Fe-coated tip under different magnet field (marked above each panel). The mapping area is the same for these panels (size: 46×20 nm 2 , $V_b = -100$ mV, $I = 80$ pA, $\Delta V = 10$ mV). (e) averaged line profile (along X direction) of panel (a) and (c). A phase inversion can be clearly seen for $B_x = \pm 1$ T. (f) Spin contrast (polarization ratio) calculated by the relative difference of the line profile in panel (e). (g) STM image of three adjacent mono-atomic steps. The step height is ~ 1.45 Å. (h) dI/dV maps taken in the same area of (g), the SDW displays phase inversion across each step edge, as indicated by yellow and red dashed lines ($V_b = -200$ mV, $I = 100$ pA, $\Delta V = 15$ mV). (i) A sketch of local spin configuration and IC-SDW near Cr (001) surface.

Moreover, in addition to the SDW modulation, we also observed another type of

modulation with half the period of SDW (3.0 nm), as shown in the dI/dV map in Fig. 2(d) (taken at $V_b = -10$ mV). It displays the same domain structures with the SDW shown in Fig. 2(b), however here the two domains have the same contrast. We further verified that such 3.0 nm modulation is also visible under a nonmagnetic PtIr tip, but the SDW is invisible (see Fig. S2). Therefore, it is natural to assign such spin-unpolarized modulation to CDW with a $\mathbf{Q}_{\text{CDW}} = 2\mathbf{Q}_{\text{SDW}}$, as reported in X-ray studies of Cr [10,13]. We noticed a previous STM study on Cr (110) surface reported similar charge modulation that originated from bulk CDW [27]. Here we are able to image the SDW and CDW simultaneously, enabling the study of their microscopic correlations, as discussed below.

Figs. 4(a~h) show a series of dI/dV maps taken in the same region, with the same Cr tip but at various V_b 's. Their (averaged) line profiles are summarized in Fig. 4(j), which display the evolution of SDW/CDW modulations as the energy varies. Fig. 4(i) shows the typical dI/dV spectrum of this mapping region, and the energy positions corresponding to line profiles in Fig. 4(j) are indicated by dashed lines. The SDW modulation is mainly observable in the energy range of -200 meV \sim -50 meV, which covers the large DOS peak in dI/dV . This suggests the peak is from certain spin-polarized state(s). As the mapping energy lowered to -50 meV \sim 0 , the 3.0 nm CDW modulation became pronounced. Interestingly, it displays an abrupt phase inversion between -30 meV and -10 meV (see also the dI/dV maps in Fig. 4(f) and 4(g)). Such π phase shift can also be seen in the phase of their Fourier transformation, as shown in Fig. 4(k). We note this energy range exactly covers the DOS dip in the dI/dV spectrum (Fig. 4(i)), which strongly suggests such a DOS dip is from a CDW gap, as the phase inversion of particle-hole states around the gap is a hallmark of CDW [36,37]. However, it is remarkable that the gap is not opened at E_F here, but ~ 22 meV below, which is rather unexpected for conventional CDW [1]. This gap is also unlikely associated with the SDW as its size (~ 10 meV) is too small compared to the Neel temperature of Cr ($T_N = 311$ K). We note in previous ARPES study on Cr (110), a SDW gap is found to be about 200 meV and located above E_F [14], which can be understood through AFM coupling induced band folding (as the hole pocket of Cr is larger than electron pocket, their crossing point upon folding is above E_F). However, here we did not observe an obvious SDW gap in tunneling spectrum, although the tunneling conductance at positive energy is indeed low in Fig. 1(f) (whether it is related to SDW gap needs further investigation). Based on the same electronic structure, a CDW gap below E_F cannot be induced by the band folding scenario either. It therefore suggests the formation of CDW is beyond the intuitive Fermi surface nesting picture.

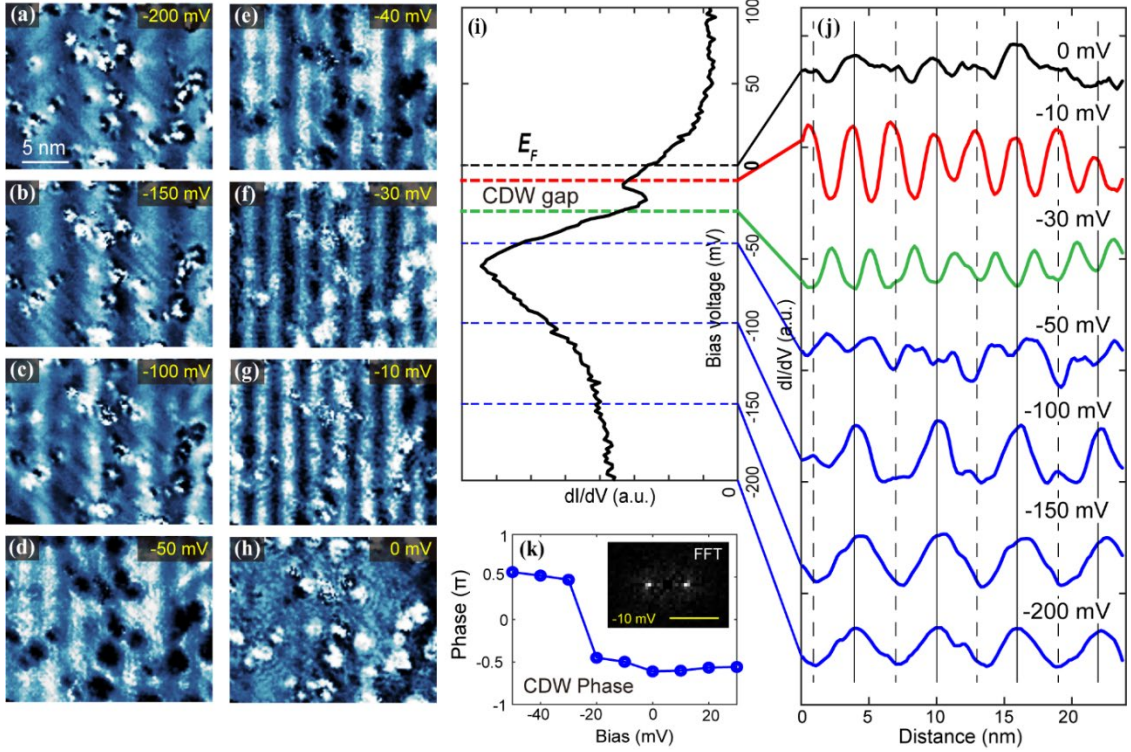


Figure 4. Evolvement of SDW/CDW modulations with energy, and the phase inversion of CDW. (a~h) dI/dV maps taken by Cr-coated tip at various V_b . The mapping area are the same for these panels. (i) averaged line profile of the dI/dV maps. An abrupt phase inversion can be seen between $V_b = -30$ and -10 mV, which corresponds to the DOS dip region in (j). (j) The typical dI/dV spectrum taken in this region. (k) The phase of the CDW modulation extracted from the scattering spots in FFT (inset image).

Further information can be extracted from the real space imaging of SDW and CDW is their phase relation. As discussed before, the SDW modulations in dI/dV are directly induced by spin contrast (Fig. 3). Their maximum and minimum positions are where the absolute spin density reach maximum. Meanwhile, the CDW modulation in dI/dV is the local DOS variation induced by periodic charge distribution [36]. Fig. 4(j) shows that the locations with maximum spin density (tracked by solid and dashed lines) always have minimum LDOS at -30 mV and maximum LDOS at -10 meV. As usually the charge density is proportional to the LDOS of occupied state near E_F , our data suggests the SDW and CDW in Cr are *in-phase*, i.e., the positions with maximum spin density also have maximum charge density (sketched in Fig. 1(b)). We note that previously such relation can only be obtained through combined X-ray and neutron diffraction measurement after extensive data analysis [38,39], while here we provide a rather direct evidence on the same system. The in-phase relation appears to consist with the theory which treat CDW as a second harmonics of SDW [12,40].

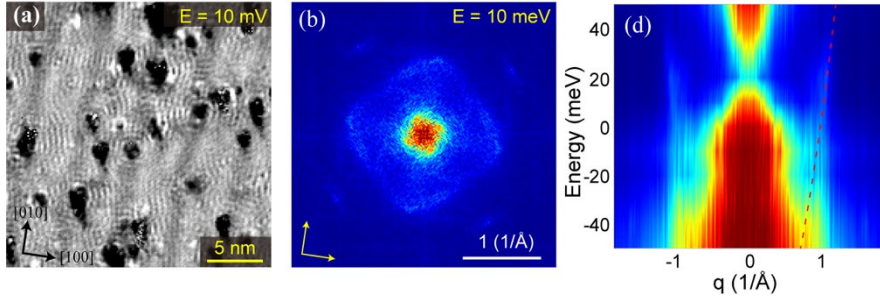


Fig. 5 QPI measurement on Cr (001) surface. (a) dI/dV image taken at $V_b = 10$ mV ($I = 100$ pA), which shows the QPI modulation. (b) The four-fold symmetrized FFT image of at $E = 10$ meV. The dashed circle indicated the FFT spots from c(2×2) reconstruction. (c) Color plot of the summarized FFT line cuts, dashed line tracks the dispersion of electron-like band.

At last, beside the static SDW/CDW modulations, we also observed dispersive quasi-particle interference (QPI) on the surface. As shown in Fig. 5(a) for example, clear short wavelength interference patterns are visible around the defects. Fig. 5(b) is the fast-Fourier transform (FFT) of Fig. 5(a) which displays a square shaped scattering ring (see Fig. S3 for more QPI data). By summarizing the FFTs taken at various energies (Fig. 5(c)), an electron-like dispersion with $q_F \sim 1.1 \text{ \AA}^{-1}$ is visualized. We note previous DFT calculations had predicted multiple spin-polarized surface states on Cr(001) [33], the observed QPI could be originated from one of the surface states (bulk bands usually do not generate strong QPI); and the DOS peak at $E \sim -75$ meV in dI/dV (Fig. 1(f)) could be from the onset of this band. The clear observation of QPI here (which is absent in previous STM studies) is also an indication of improved surface condition. We expect it will help to elucidate the surface electronic states of Cr with the help of further theoretical calculations.

We have now presented a comprehensive SP-STM study on a well-ordered Cr(001) surface. We directly observed the incommensurate SDW with similar spin configurations to the bulk, which manifests as long-period, pure spin modulations on the surface, and the coexisting CDW order is also simultaneously observed. These features are absent in previous STM studies which indicates the surface condition is important for probing intrinsic magnetism of Cr. Another main finding of this work is the CDW gap opened below E_F . It appears conflict with conventional Fermi surface nesting picture in which the density wave gap will open at E_F to lower the energy. Nonetheless, if considering the CDW in Cr is driven by SDW [12,40], the system would gain energy mainly through SDW, and it is possible the formation of CDW involves states away from E_F . This implies additional factors, such as electron correlations, may play a role in CDW of Cr. Moreover, as a real space measurement, we can directly observe the domain and phase relations of SDW and CDW. The same domain structure and an in-phase relation of local spin and charge indicate these two orders are highly correlated, consistent with the scenario that CDW is the high-order harmonics of SDW.

The mechanism of coexisting spin/charge orders has long been an important issue in

condensed matter physics, particularly for correlated materials such as cuprates [3,41] and iron-based superconductors [42], our new spectroscopic and microscopic information provide new insights on the comprehensive understanding SDW/CDW in Cr and other correlated materials. Furthermore, our work demonstrates the ability of simultaneous imaging these orders with high resolution. We expected similar SP-STM measurement shall also be applied to other systems and would inspire more studies on the coexisting quantum orders.

Acknowledgment:

We thank Prof. Chunlei Gao and Mr. Zhongjie Wang for the advice of preparing spin-polarized tip and helpful discussions. This work is supported by the National Key R&D Program of the MOST of China (Grant Nos. 2017YFA0303004, 2016YFA0302300), National Natural Science Foundation of China (Grant Nos. 92065202, 11888101, 11790312, 11961160717), Science Challenge Project (grant No. TZ2016004), Shanghai Municipal Science and Technology Major Project (Grant No. 2019SHZDZX01)

***E-mail:** tzhang18@fudan.edu.cn

Reference:

- [1]. G. Gruner, *Density waves in Solids*, Addison-Wesley Publishing (1994)
- [2]. A M Gabovich et al., *Charge- and spin-density-wave superconductors*, Supercond. Sci. Technol. **14**, R1 (2001)
- [3]. S. A. Kivelson et al., *How to detect fluctuating stripes in the high-temperature superconductors*, Rev. Mod. Phys. **75**, 1201 (2003).
- [4]. P. C. Dai, J. P. Hu, and E. Dagotto, *Magnetism and its microscopic origin in iron-based high-temperature superconductors*, Nature Physics, **8**, 709 (2012)
- [5]. M. Enayat, et al., *Real-space imaging of the atomic-scale magnetic structure of $Fe_{1+y}Te$* , Science **345**, 653 (2014)
- [6]. E. Fawcett, *Spin-density-wave antiferromagnetism in Cr*. Rev. Mod. Phys. **60**, 209 (1988).
- [7]. E. Fawcett, et al. *Spin-density-wave antiferromagnetism in chromium alloys*. Rev. Mod. Phys. **66**, 25 (1994).
- [8]. H. Zabel, *Magnetism of chromium at surfaces, at interfaces and in thin films*. J. Phys. Condens. Matter **11**, 9303 (1999).
- [9]. A. W. Overhauser, *Spin density waves in an electron gas*. Phys. Rev. **128**, 1437 (1962).
- [10]. Doon Gibbs and K. M. Mohanty, *High-resolution x-ray-scattering study of charge-density-wave modulation in chromium*, Phys. Rev. B. **37**, 562 (1988)
- [11]. Tsunoda, Y., M. Mori, N. Kunitomi, Y. Teraoka, and J. Kanamori, *Strain wave in pure chromium*. Solid State Commun. **14**, 287 (1974)
- [12]. C.Y. Young and J. B. Sokoloff, *The role of harmonics in the first order antiferromagnetic to*

paramagnetic transition in chromium J. Phys. F **4**, 1304 (1974).

[13].J. P. Hill, G. Helgesen, Doon Gibbs, *X-ray-scattering study of charge- and spin-density waves in chromium*, Phys. Rev. B. **52**, 7363 (1995)

[14].J. Schäfer, Eli Rotenberg, G. Meigs, and S. D. Kevan, *Direct Spectroscopic Observation of the Energy Gap Formation in the Spin Density Wave Phase Transition at the Cr(110) Surface*, Phys. Rev. Lett. **83**, 2069 (1999)

[15].E. Rotenberg, *et al.* *Electron states and the spin density wave phase diagram in Cr(110) films*. New J. Phys. **7**, 114 (2005).

[16].R. Wiesendanger, *Spin mapping at the nanoscale and atomic scale*, Rev. Mod. Phys. **81**, 1495 (2009).

[17].R. Wiesendanger, *et al.* *Observation of vacuum tunneling of spin-polarized electrons with the scanning tunneling microscope*. Phys. Rev. Lett. **65**, 247 (1990).

[18].M. Kleiber, *et al.* *Topology-induced spin frustrations at the Cr(001) surface studied by spin-polarized scanning tunneling spectroscopy*. Phys. Rev. Lett. **85**, 4606 (2000).

[19].T. Hänke, *et al.* *Absence of spin-flip transition at the Cr(001) surface: A combined spin-polarized scanning tunneling microscopy and neutron scattering study*. Phys. Rev. B **71**, 184407 (2005).

[20].M. Kleiber, *et al.* *Magnetic properties of the Cr(001) surface studied by spin-polarized scanning tunneling spectroscopy*. J. Magn. Magn. Mater. **240**, 64 (2002).

[21].T. Kawagoe *et al.*, *Evidence of a topological antiferromagnetic order on ultrathin Cr(001) film surface studied by spin-polarized scanning tunneling spectroscopy*, J. Appl. Phys. **93**, 6575–6577 (2003)

[22].H. Oka, and K. Sueoka, *Spin-polarized scanning tunneling microscopy and spectroscopy study of c(2×2) reconstructed Cr(001) thin film surfaces*. J. Appl. Phys. **99**, 08D302 (2006).

[23].B. Santos, *et al.* *Structure and magnetism of ultra-thin chromium layers on W(110)*. New. J. Phys. **10**, 013005 (2008).

[24].J. Lagoute, *et al.* *Spin-polarized scanning tunneling microscopy and spectroscopy study of chromium on a Cr(001) surface*. J. Phys. Condens. Matter **23**, 045007 (2011).

[25].P. J. Hsu, *et al.* *Observation of a spin-density wave node on antiferromagnetic Cr(110) islands*. Phys. Rev. B **87**, 115437 (2013).

[26].J. P. Corbett, A. R. Smith, *Applying a difference ratio method in spin-polarized scanning tunneling microscopy to determine crystalline anisotropies and antiferromagnetic spin alignment in Cr(001) c(2×2)*, Journal of Magnetism and Magnetic Materials **465**, 626–633 (2018)

[27].K. F. Braun, *et al.* *Observation of charge-density wave domains on the Cr(110) surface by low-temperature scanning tunneling microscopy*. Phys. Rev. Lett. **85**, 3500 (2000).

[28].G. Allan, *Surface electronic structure of antiferromagnetic chromium*, Surf. Sci. **74**, 79 (1978)

[29].H. C. Jeong and E. D. Williams, *Steps on surfaces: experiment and theory*, Surf. Sci. Rep. **34**, 171-294 (1999).

[30].M. Schmid, *et al.* *Segregation of impurities on Cr(100) studied by AES and STM*. Surf. Sci. **377-379**, 1023 (1997).

[31].J. A. Stroscio, *et al.* *Tunneling spectroscopy of bcc (001) surface states*. Phys. Rev. Lett. **75**, 2960 (1995).

[32].O. Yu. Kolesnychenko, *et al.* *Real-space imaging of an orbital Kondo resonance on the Cr(001) surface*. Nature **415**, 507 (2002).

[33].P. Habibi, *et al.* *Electronic and magnetic structure of the Cr(001) surface*. J. Phys. Condens. Matter **25**, 146002 (2013).

[34].M. A. Leroy, *et al.* *Electronic structure of the Cr(001) surface and Cr/MgO interface*. Phys. Rev. B **88**, 205134 (2013).

- [35]. M. Budke, T. Allmers, and M. Donath, *Surface state vs orbital Kondo resonance at Cr(001): Arguments for a surface state interpretation*, Phys. Rev. B 77, 233409 (2008)
- [36]. W. Sacks, D. Roditchev, and J. Klein, *Voltage-dependent STM image of a charge density wave*, Phys. Rev. B 57, 13118 (1998).
- [37]. P. Mallet, K. M. Zimmermann, P. Chevalier, J. Marcus, J. Y. Veuillen, and J. M. G. Rodriguez, *Contrast reversal of the charge density wave STM image in purple potassium molybdenum bronze K0.9Mo6O17*, Phys. Rev. B 60, 2122 (1999).
- [38]. Y. Tsunoda, Y. Nakai, N. Kunitomi, *Phase relation between SDW and strain wave in chromium*, Solid State Communications, 16, 443-445 (1975)
- [39]. M. Mori, *et al.* *Searching for charge density waves in chromium*. J. Phys. Condens. Matter **5**, L77 (1993).
- [40]. X. W. Jiang and R. S. Fishman, *Coupled spin- and charge-density waves in chromium alloys*, J. Phys.: Condens. Matter 9, 3417–3426 (1997)
- [41]. Ying Zhang *et al.*, *Competing orders in a magnetic field: Spin and charge order in the cuprate superconductors*. Phys. Rev. B, 66, 094501 (2002)
- [42]. A. V. Balatsky, D. N. Basov, and J. X. Zhu *Induction of charge density waves by spin density waves in iron-based superconductors* Phys. Rev. B 82, 144522 (2010)

Supplementary materials of Real-space Observation of Incommensurate Spin Density Wave and Coexisting Charge Density Wave on Cr(001) surface

This supplementary material contains additional data set taken by spin-polarized tip and normal tip. Details can be found in the figure caption.

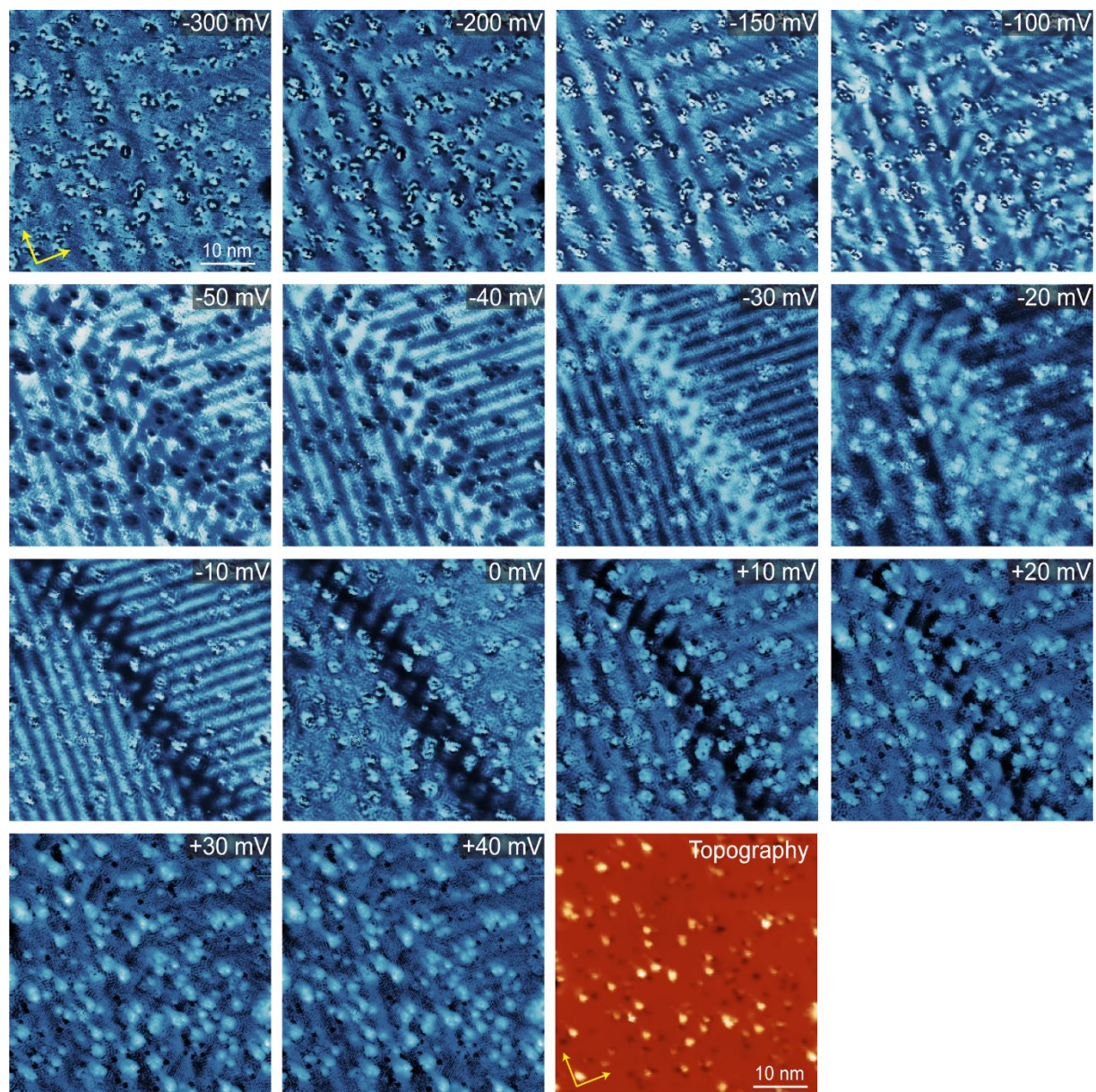


Figure S1. A set of dI/dV maps taken at various energies with a 30 nm thick Cr coated tip. The mapping energy is labeled in each panel. The last panel is the topographic image of the mapping area. Two SDW/CDW domains can be seen in dI/dV maps, while the domain structure is unrelated to topography.

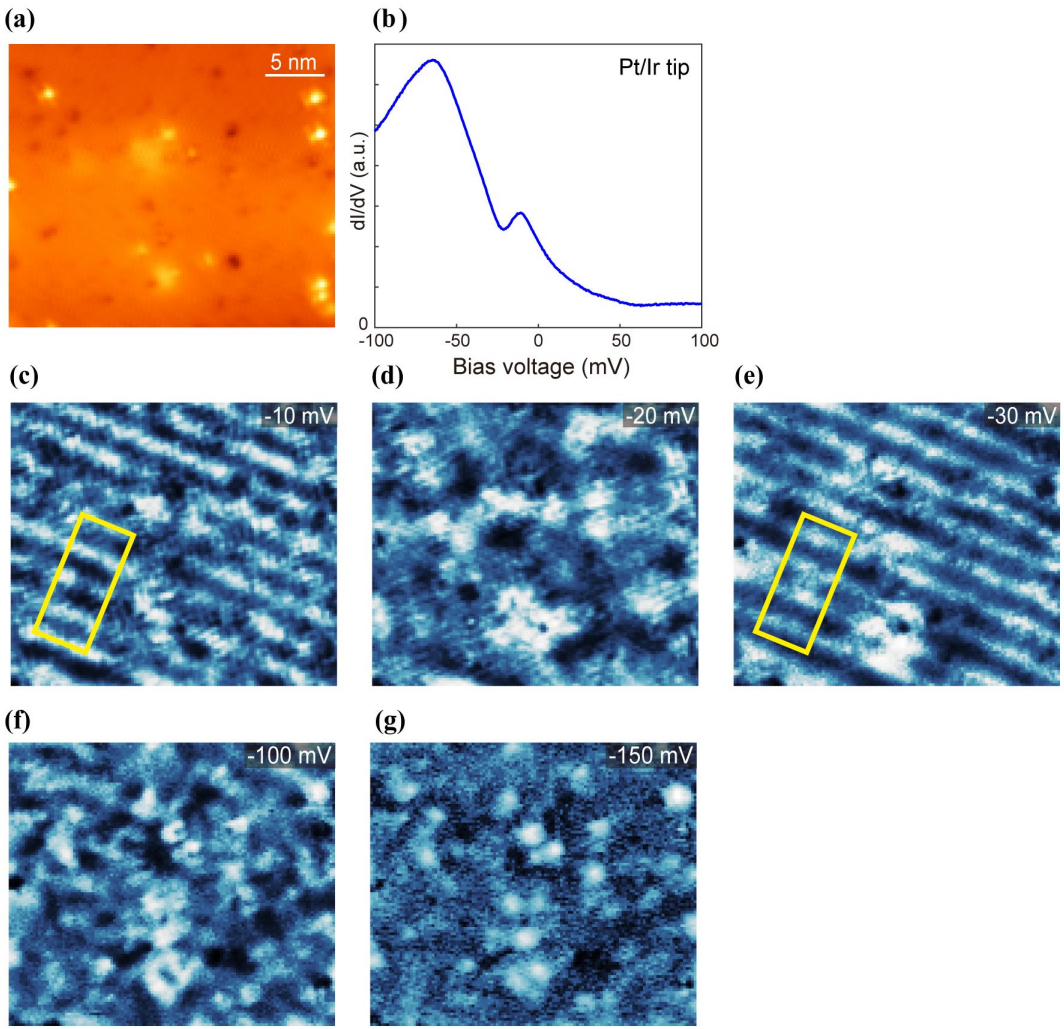


Figure S2. A data set measured by a normal PtIr tip. (a) Topographic image of Cr(001) ($29 \times 25 \text{ nm}^2$). (b) dI/dV spectrum taken by the PtIr tip, which also displays a DOS dip (CDW gap) at $\sim 20 \text{ meV}$ and a peak at $\sim -70 \text{ meV}$. (c~f) dI/dV maps taken in the same area as that shown in panel (a). The mapping energy are labelled in each panel. The 3.0 nm period CDW modulations are still present at energies close to E_F , but the SDW modulations are absent in all the maps. The CDW phase inversion between -30 meV and -10 meV can also be seen, as indicated by the rectangles at the same position in panel (c) and (e). The modulations in these rectangles are out-of-phase. Note there is no modulation at $E = -20 \text{ meV}$ as it is in the gap center.

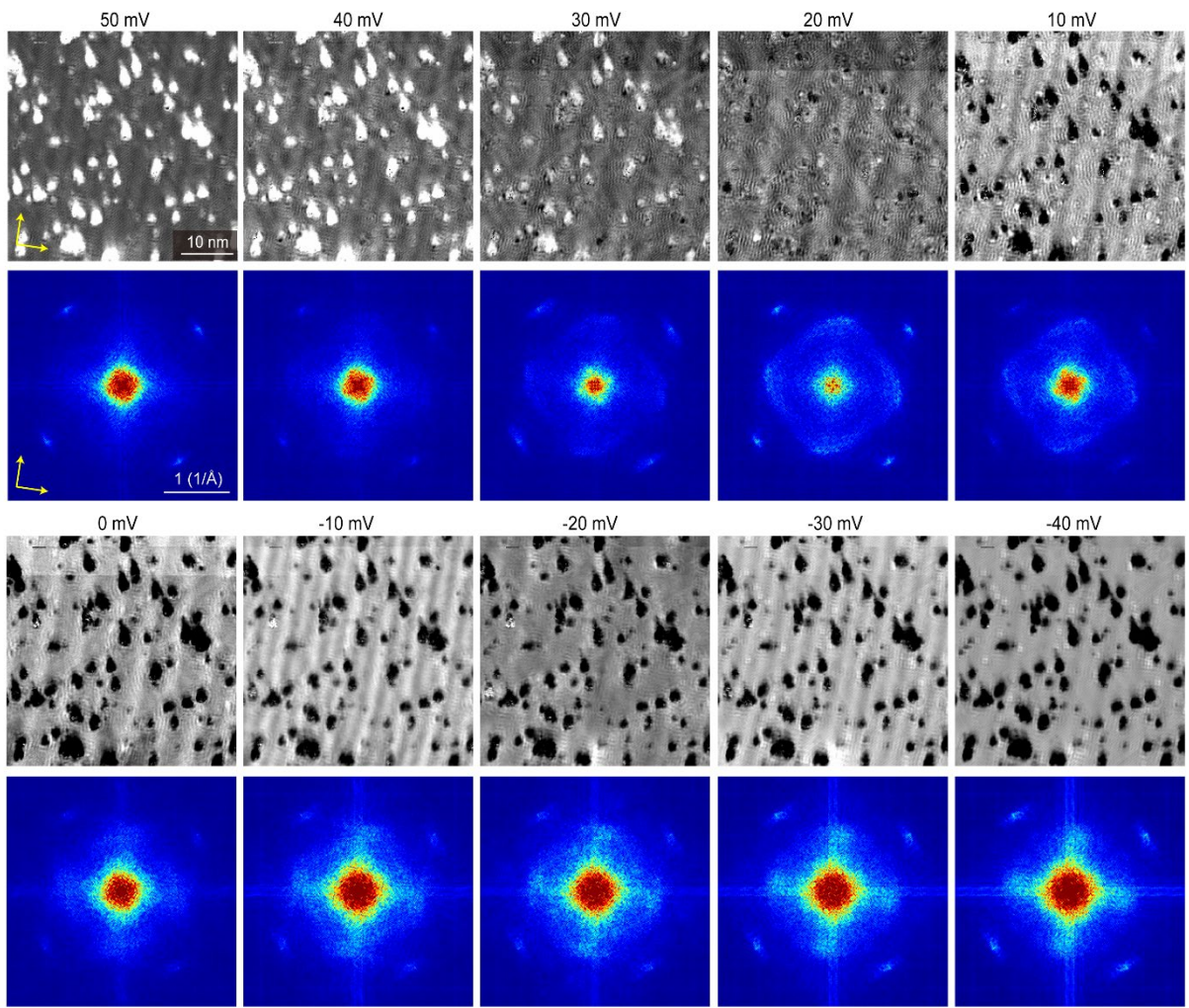


Figure S3. QPI measurement: A set of dI/dV maps and corresponding FFT images taken by a Cr tip, which show QPI patterns together with the SDW/CDW modulations. The mapping energy is labeled in each panel.